Mathematical Biosciences and Engineering

MBE, 21(1): 144–169.
DOI: 10.3934/mbe.2024007
Received: 14 August 2023
Revised: 22 November 2023
Accepted: 03 December 2023
Published: 11 December 2023

http://www.aimspress.com/journal/MBE

Research article

A new fractional fuzzy dispersion entropy and its application in muscle fatigue detection

Baohua Hu[1], Yong Wang[2,*] and Jingsong Mu[2,3]

[1] School of Advanced Manufacturing Engineering, Hefei University, Hefei 230601, China
[2] School of Mechanical Engineering, Hefei University of Technology, Hefei 230009, China
[3] Department of Rehabilitation Medicine, The First Affiliated Hospital of USTC, Division of Life Sciences and Medicine, University of Science and Technology of China, Anhui Provincial Hospital, Hefei 230036, China

* **Correspondence:** Email: simenkouwang@sina.com.

Abstract: Recently, fuzzy dispersion entropy (DispEn) has attracted much attention as a new nonlinear dynamics method that combines the advantages of both DispEn and fuzzy entropy. However, it suffers from limitation of insensitivity to dynamic changes. To solve this limitation, we proposed fractional fuzzy dispersion entropy (FFDispEn) based on DispEn, a novel fuzzy membership function and fractional calculus. The fuzzy membership function was defined based on the Euclidean distance between the embedding vector and dispersion pattern. Simulated signals generated by the one-dimensional (1D) logistic map were used to test the sensitivity of the proposed method to dynamic changes. Moreover, 29 subjects were recruited for an upper limb muscle fatigue experiment, during which surface electromyography (sEMG) signals of the biceps brachii muscle were recorded. Both simulated signals and sEMG signals were processed using a sliding window approach. Sample entropy (SampEn), DispEn and FFDispEn were separately used to calculate the complexity of each frame. The sensitivity of different algorithms to the muscle fatigue process was analyzed using fitting parameters through linear fitting of the complexity of each frame signal. The results showed that for simulated signals, the larger the fractional order q, the higher the sensitivity to dynamic changes. Moreover, DispEn performed poorly in the sensitivity to dynamic changes compared with FFDispEn. As for muscle fatigue detection, the FFDispEn value showed a clear declining tendency with a mean slope of -1.658×10^{-3} as muscle fatigue progresses; additionally, it was more sensitive to muscle fatigue compared with SampEn (slope: -0.4156×10^{-3}) and DispEn (slope: -0.1675×10^{-3}). The highest accuracy of 97.5% was achieved with the FFDispEn and support vector machine (SVM). This study

provided a new useful nonlinear dynamic indicator for sEMG signal processing and muscle fatigue analysis. The proposed method may be useful for physiological and biomedical signal analysis.

Keywords: complexity analysis; fractional fuzzy dispersion entropy; fractional calculus; muscle fatigue; sEMG signal

1. Introduction

Signal complexity analysis in biomedical engineering applications is becoming increasingly important and a study focus for scholars [1]. Different methods have been proposed to measure the complexity of different types of complicated non-stationary nonlinear signals, such as entropy algorithms, Lyapunov exponents and fractal dimensions [2–4]. Among these methods, entropy algorithms are the most popular because of their effectiveness and ease of operation. Approximate entropy (ApEn) is a nonlinear dynamic indicator to measure the complexity and regularity of signals [5]. However, ApEn counts each sequence as self-matching, and this may lead to a bias in calculation results [6]. Richman and Moorman [7] proposed sample entropy (SampEn) to relieve the bias caused by self-matching. SampEn eliminates self-matching and demonstrates less dependence on data length and better relative consistency. However, SampEn is constructed based on a step function that classifies all cases into zero or one. It is unreasonable to categorize an input as either zero or one in the real physical world. To solve the above-mentioned problems, Xie et al. proposed fuzzy entropy based on SampEn and a fuzzy membership function [8]. Compared with SampEn, fuzzy entropy has better anti-noise performance and signal length robustness, and it has been successfully applied in biomedical and neuroelectrophysiological signal processing.

Rostaghi et al. proposed dispersion entropy (DispEn) by combining the Shannon entropy and dispersion pattern [9]. Compared with the existing methods, DispEn has the following advantages: (1) DispEn will not have undefined results when processing short-time signals; (2) DispEn has better robustness to noise; (3) DispEn is faster, especially compared to SampEn [10–12]. Because of these advantages, DispEn has been successfully applied in different scientific and engineering fields, including biomedical engineering, mechanical engineering and computer engineering [13–16]. In the calculation step of DispEn, the initial time series is finally mapped (quantized) to a series of integers after different mathematical transformations and named as class [9]. This mapping step (quantization step) uses an integer function that is similar to the Heaviside function employed in SampEn; this integer function may cause some useful information in the data to be eliminated. This characteristic makes DispEn sensitive to parameter selection and signal length, as well as SampEn. In addition, small changes in the amplitude of the time series due to noise can also change the quantization sequence and, thus, change the entropy.

To solve this problem, Rostaghi et al. proposed fuzzy DispEn for the first time and verified its advantages over DispEn [17]. However, fuzzy DispEn has the disadvantage of being insensitive to dynamic changes. Hence, it is essential to further optimize the method so as to detect dynamic changes more precisely. For fuzzy membership function, this paper proposes a new computing method based on Euclidean distance. For dynamic changes detection sensitivity, Li et al. proposed coded dispersion entropy (CDE) and simplified coded dispersion entropy (SCDE) to improve their performance in detecting nonlinear dynamic changes [18]. Their results show that CDE and SCDE are more sensitive

to dynamic changes in time series. Moreover, another way to improve sensitivity is to use fractional calculus [19]. Research on the application of fractional calculus to entropy has been conducted by many scholars [20]. In this study, we use fractional calculus to improve sensitivity in detecting dynamic changes.

With the in-depth study of complex systems, the theory of fractional calculus has attracted wide attention from scholars in recent decades and it has been successfully applied to engineering, physics, system control and other fields. Fractional calculus has become a research hotspot [19–21]. Furthermore, the fractional entropy metric was proposed by combining fractional calculus and the entropy theory of information [22]. Fractional entropy has been successfully applied in the detection of dynamic complexity change [4,22]. Motivated by previous works, the present study proposes a new fractional entropy metric based on DispEn, a fuzzy membership function and fractional calculus. We hope that the fuzzy membership function can solve the inherent defects of DispEn and that fractional calculus can improve the sensitivity of the entropy metric to dynamic changes.

Muscle fatigue detection has always been a topic of interest in biomedical engineering research [23–26]. Muscle fatigue is the inability of muscles to maintain a required force during continuous contraction and is a common occurrence in human activities [27]. Excessive muscle fatigue significantly increases the risk of neuromuscular disorders and decreases the stability of rehabilitation training [28]. The functional state of nerves and muscles can be reflected by surface electromyography (sEMG) signal. Hence, sEMG is considered as one of the most effective tools to study muscle fatigue [29–31]. Most of the existing research focuses on time-domain analysis and frequency-domain analysis of sEMG signals. The amplitude of sEMG signals will rise and the signal spectrum will shift to the left as muscle fatigue [32,33]. The most commonly used indicators in such analyses are the mean power frequency and median frequency [34,35]. However, some studies have shown that the median frequency is less reliable than SampEn, fuzzy ApEn and other nonlinear indices when evaluating muscle fatigue [36]. Hence, an effective nonlinear metric based on entropy for muscle fatigue analysis still needs to be established.

With the development of artificial intelligence (AI), many AI methods have been used for biomedical signal processing and muscle fatigue detection, such as multilayer perceptron (MLP), logistic regression (LR), K nearest neighbors (KNN), support vector machine (SVM), convolutional neural network-support vector machine (CNN-SVM), convolutional neural network-long short-term memory (CNN-LSTM) and graph neural network (GNN) [37–44]. Murillo-Escobar et al. used permutation entropy (PE) and logistic regression to classify three states of muscle fatigue progression with an accuracy of 80% [38]. Jero et al. constructed an upper limb muscle fatigued recognition model based on geometric features of sEMG signals, achieving a highest accuracy of 86% with MLP [39]. Karthick et al. adopted high-resolution time-frequency features of sEMG signals and obtained an accuracy of 91% using SVM in dynamic muscle fatigue detection [40]. Wang et al. adopted a CNN and three types of commonly used statistical algorithms for sEMG signal features extraction, achieving an accuracy of 96.5% in muscle fatigue detection using SVM [41]. Wang et al. performed LSTM network for lower limb muscle fatigue state recognition and obtained an accuracy of 95.19% in classifying muscle non-fatigue and fatigue states [42]. Shoeibi et al. obtained an accuracy of 99.43% in automatic schizophrenia diagnosis using functional connectivity features and the CNN-LSTM model [43]. In summary, both deep learning and traditional machine learning have been used in biomedical signals processing and muscle fatigue detection and have achieved effective results [44]. Although deep learning-based methods can improve the accuracy of muscle fatigue detection, the

increased computational complexity and more computational resources with hardware dependency may limit their application in the field of real-time monitoring [45]. One application of the muscle fatigue detection is to avoid secondary injury of stroke patients by real-time muscle state monitoring in rehabilitation training [46]. Traditional machine learning methods have the advantage of interpretability and low computational complexity compared to deep learning, making them valuable tools for muscle fatigue detection [44]. SVM has been demonstrated to give the best performance considering the balance of computational complexity and detection accuracy [47]. Hence, to further evaluate the performance of extracted entropy metric in muscle fatigue detection, SVM was used to classify non-fatigue and fatigue conditions in this study.

In summary, we propose fractional fuzzy dispersion entropy (FFDispEn) based on DispEn, a fuzzy membership function and fractional calculus in this study. First, a threshold is set based on the Euclidean distance between the embedding vector and dispersion pattern. Within the threshold's range, the fuzzy membership function is used to replace the integer function employed in DispEn to determine the fuzzy membership degree of the embedding vector and dispersion pattern. According to this fuzzy membership degree, the probability of each dispersion pattern is then determined. After the fuzzy DispEn is obtained, we utilize fractional calculus to obtain FFDispEn. Simulated signals generated by the one-dimensional (1D) logistic map and sEMG signals are used to test algorithm performance. We hope this study can provide a new nonlinear index that can reflect complexity changes precisely so as to provide a new method for muscle fatigue detection.

2. Materials and methods

2.1. System design

In this study, an sEMG acquisition system for muscle fatigue detection was developed. The sEMG signals were acquired through a hardware circuit system including a simple filter circuit and an ADS1299, which is a 24-bit analog-to-digital converter, then the processed sEMG signals were received by an STM32F103C8 chip, which is a 32-bit microprocessor based on ARM Cortex-M3 core, through serial communication. The biceps brachii was selected for electrode placement. sEMG signals were measured using bipolar electrodes placed on the biceps brachii muscle with respect to a common reference electrode placed on a location that has no muscle activity. Considering that the sEMG frequency is concentrated at 15–500 Hz, the signal sampling frequency of the sEMG acquisition system was 1000 Hz [48].

2.2. Subjects, experimental procedures, and data acquisition protocol

A muscle fatigue detection experiment was conducted at Hefei University. This study was approved by the Ethics Review Committee of Hefei University of Technology, China and performed in accordance with the Declaration of Helsinki. All subjects were required to read experimental instructions and provide written informed consent before the experiment. A total of 29 healthy volunteers (all males; 20.9 ± 0.6 years old; age range 19–22 years) were recruited for the muscle fatigue detection study.

Before the experiment, the subject's biceps brachii muscle was wiped carefully with alcohol to ensure good electrical contact between the skin and electrodes. To avoid interference from external

factors such as temperature, the experiment was arranged in a quiet, closed room with the temperature set at 26 °C. Subjects had the right to withdraw from the research at any time. Two disposable sEMG Ag/AgCl differential electrodes were placed at the muscle belly of the biceps brachii. The distance between two electrodes was two cm [49]. The reference electrode was placed at the elbow joint where there is no muscle activity. During the experiment, all subjects were required to stand up straight with their upper arms parallel to their bodies. They held a five kg dumbbell with their forearms and upper arms at 90° until exhaustion, as shown in Figure 1. The sEMG signals were recorded for the entire duration of the experiment.

Figure 1. Muscle fatigue experiment.

2.3. sEMG signal de-noising based on variational mode decomposition (VMD)

Low-magnitude sEMG signals can easily be contaminated by two main types of noise: Baseline wander noise and white Gaussian noise. Signal filtering is essential before feature value extraction so as to prevent useful information from being drowned by noise and to extract as much useful information as possible. We propose a signal de-noising procedure based on variational mode decomposition (VMD) [50].

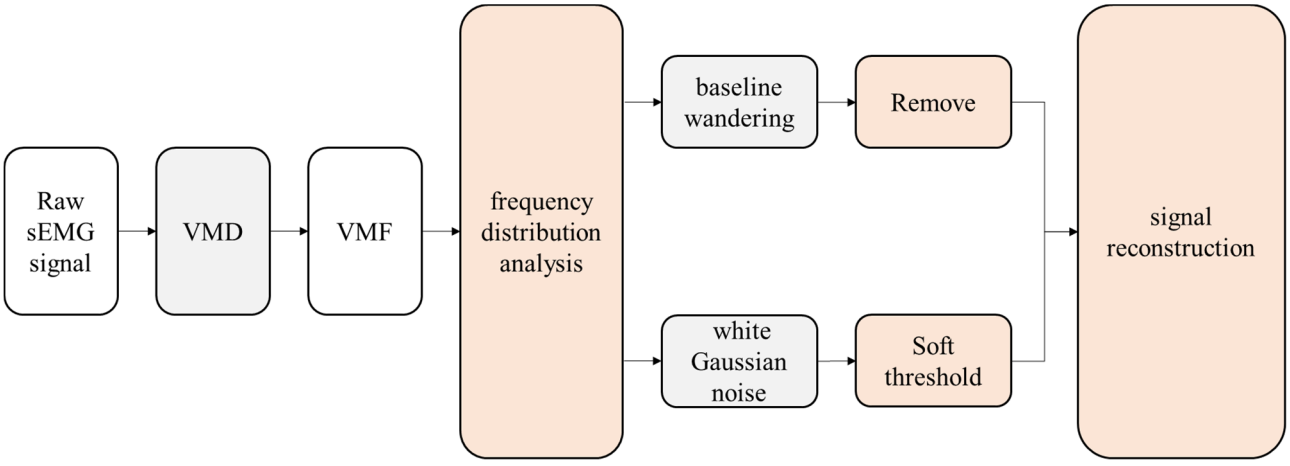

Figure 2. Flow diagram of the proposed denoising algorithm based on VMD.

First, the noisy sEMG signal is decomposed into an ensemble of band-limited modes of different frequency bands, which is called variational mode function (VMF). This step is completed based on

VMD. The key parameter of VMD is the number of decomposition modes K. To completely separate the noise, parameter K needs to be set as large as possible. However, the computational complexity will increase with a large parameter setting [51]. Therefore, we set K to 10 in order to balance the computational complexity and de-noising accuracy [50]. Other parameters in VMD, such as the penalty factor α, noise tolerance parameter τ and the tolerance of convergence criterion, were set in accordance with the literature [51]. The algorithm flow is shown in Figure 2.

Based on the frequency characteristics of noise signals, de-noising for each type of noise mentioned above is conducted in a specific mode and removed separately from the sub-band. The frequency of baseline wander in sEMG is normally less than 10 Hz [52]. Therefore, baseline wander noise tends to be restricted in the first VMF according to the characteristics of VMD. As a consequence, the first VMF in the low-frequency part of the signal is removed so as to eliminate the baseline wander noise. As for white Gaussian noise, this paper adopts a soft threshold for each VMF to remove the corresponding noise component [53]. The soft noise is set as follows:

$$f(y) = \begin{cases} \text{sgn}(y)(|y| - T), & |y| > T \\ 0, & |y| \le T. \end{cases} \tag{1}$$

Here, the value of T should be greater than the maximum noise level present in the noisy sEMG signal [54]. Hence, T can be selected as follows:

$$T = k * \sigma\sqrt{2\log_e N}, \tag{2}$$

where N is the length of the corresponding sEMG signal and σ represents the level of noise. k is an empirically set parameter. σ can be calculated as follows:

$$\sigma_i = \frac{median(|u_i(t)|)}{0.6745}. \tag{3}$$

Finally, signal reconstruction realizes noise removal.

2.4. FFDispEn

For a given time series $x = \{x_1, x_2, ..., x_N\}$ of length N, the DispEn can be obtained as outlined below.

1) x is mapped to $y = (y_1, y_2, ..., y_N)$, $y_j \in (0, 1)$ by a normal cumulative distribution function(NCDF):

$$y_j = \frac{1}{\sigma\sqrt{2\pi}} \int_{-\infty}^{x_j} e^{\frac{-(t-\mu)^2}{2\sigma^2}} dt, \tag{4}$$

where μ and σ^2 denote the expectation and variance of x, respectively.

2) Further, y is mapped to a time series u_i through linear transformation:

$$u_j^c = \text{R}\left(c * y_j + 0.5\right), \tag{5}$$

where R is the rounding function and c is the number of categories. After steps 1) and 2), each element of the time series x is mapped into [1, 2, ..., c].

3) We calculate the embedding vector using the following formula, where m is the embedding dimension and d is the time delay:

$$u_i^{m,c} = \left\{u_i^c, u_i^c, \cdots, u_i^c\right\}, i = 1, 2, \cdots, N - (m-1)d. \tag{6}$$

4) We then calculate the dispersion pattern $\pi_{v_0 v_1 \cdots v_{m-1}} (v = 1, 2, \cdots, c)$, where $u_i^c = v_0, u_{i+d}^c = v_1, \cdots, u_{i+(m-1)d}^c = v_{m-1}$. The number of possible dispersion patterns is equal to c^{m}, since all $u_i^{m,c}$ consists of m elements and each element can be one of the integers from one to c [9].

5) Next, we calculate the probability of each dispersion pattern:

$$p\left(\pi_{v_0 v_1 \cdots v_{m-1}}\right) = \frac{Number\left(\pi_{v_0 v_1 \cdots v_{m-1}}\right)}{N - (m-1)d}. \tag{7}$$

Here, $p\left(\pi_{v_0 v_1 \cdots v_{m-1}}\right)$ denotes the number of dispersion patterns of $\pi_{v_0 v_1 \cdots v_{m-1}}$ attributed to each $u_i^{m,c}$ divided by the $N - (m-1)d$ number of embedding vectors $u_i^{m,c}$.

6) Finally, according to the definition of Shannon entropy, DispEn is defined as follows:

$$\mathrm{DispEn}(x, m, c, d) = -\sum_{\pi=1}^{c^m} p\left(\pi_{v_0 v_1 \cdots v_{m-1}}\right) * \ln\left(p\left(\pi_{v_0 v_1 \cdots v_{m-1}}\right)\right). \tag{8}$$

The standardized DispEn/ln(c^m) as the DispEn entropy value was used in this study.

As can be seen from the above definition of DispEn, the rounding function assigns each member of the original series to a certain class. Such a processing method is similar to the data processing methods in SampEn. After defining the similarity tolerance r, SampEn stipulates that any distance larger than r is eliminated and only the distances that are smaller than the similarity tolerance r are retained. Therefore, both DispEn and SampEn are constructed based on the Heaviside function. However, it is illogical to categorize an input into an output, and the boundary between different classes is fuzzy in the real physical world. If the entropy is constructed by the Heaviside function, small fluctuations of an actual time series may cause sharp fluctuations in entropy. The traditional integral function of the defined DispEn will be insufficient in processing time series. For example, given the original series a = [1.5, 1.5], a will be mapped to [2, 2] according to the integral function. If the signal is weakly interfered, a = [1.499, 1.499]; then, a will be mapped to [1, 1]. Therefore, even small signal fluctuations could cause sharp fluctuations in entropy, which makes the DispEn particularly sensitive to parameter settings and noise.

Therefore, this paper uses a fuzzy membership function instead of a rounding function to define the membership degree of each dispersion pattern to embedding vectors. According to fuzzy mapping, a given vector can be assigned to multiple classes at the same time, thus avoiding the above problem caused by the Heaviside function. In accordance with the definition of Shannon entropy, the membership function should meet the following conditions. First, the sum of membership degrees of different classes should be equal to one; second, the probability of each pattern should be equal so that a random signal could have the maximum entropy theoretically [9]. Therefore, the fuzzy membership function used has equal relative cardinality for random sequences so that classes can have equal probabilities [17].

In view of the above rules, this paper adopts the following fuzzy function based on Euclidean

distance. y_j is not mapped to the range of [1, 2, ..., c] by the rounding function. Instead, we utilize the Euclidean distance to set the fuzzy membership degree. In step 2) above, compared with the DispEn that maps y to the range of [1, 2, ..., c] by taking the rounding function, this study adopts the fuzzy mapping function as described in the three steps below:

1) By linear transformation:

$$z_j^c = \left(c * y_j + 0.5\right) \tag{9}$$

This step maps y_j to $c*y_j + 0.5$.

2) We calculate the dispersion pattern $\pi_{v_0 v_1 \cdots v_{m-1}}\left(v = 1, 2, \cdots, c\right)$, where $u_i^c = v_0, u_{i+d}^c = v_1, \cdots, u_{i+(m-1)d}^c = v_{m-1}$. The number of possible dispersion patterns is equal to c^{m}, since all $u_i^{m,c}$ consists of m elements and each element can be one of the integers from one to c [9].

3) We then calculate the probability of each dispersion pattern. Different from DispEn, this study defined the embedding vector, embd(i) = z(i : i+(m-1)*d), i = 1: N-(m-1)*d. After the definition, the Euclidean distance between the embedding vector and the dispersion pattern is calculated, and the dispersion pattern whose Euclidean distance is less than the threshold value r is selected. The probability of the occurrence of the corresponding dispersion pattern is allocated according to the size of Euclidean distance.

If for embedding vector z(l: l+(m-1)*d), there are k dispersion patterns whose Euclidean distance is less than r and the distance matrix dis(k) is obtained. The probability of each dispersion pattern is shown as follows:

$$p\left(\pi_{v_0 v_1 \cdots v_{m-1}}\right)\Big|_{z(l:l+(m-1)*d)} = \frac{r - dis(i)}{k * r - sum(dis)}. \tag{10}$$

Furthermore, the probability of each dispersion mode is calculated as follows:

$$p\left(\pi_{v_0 v_1 \cdots v_{m-1}}\right) = \frac{sum\left(p\left(\pi_{v_0 v_1 \cdots v_{m-1}}\right)\Big|_{z(l:l+(m-1)*d)}\right)}{N-(m-1)d}. \tag{11}$$

4) Based on the definition of Shannon entropy, Fuzzy-DispEn is defined as:

$$\text{Fuzzy-DispEn}\left(x, m, c, d\right) = -\sum_{\pi=1}^{c^m} p\left(\pi_{v_0 v_1 \cdots v_{m-1}}\right) * \ln\left(p\left(\pi_{v_0 v_1 \cdots v_{m-1}}\right)\right). \tag{12}$$

5) Finally, based on fractional calculus, FFDispEn is defined as:

$$\begin{aligned} &\text{FFDispEN}\left(x, m, c, d, q\right) = \\ &-\sum_{\pi=1}^{c^m} p\left(\pi_{v_0 v_1 \cdots v_{m-1}}\right)\left\{\frac{p\left(\pi_{v_0 v_1 \cdots v_{m-1}}\right)^{-q}}{\Gamma\left(1+q\right)}\left[\ln\left(p\left(\pi_{v_0 v_1 \cdots v_{m-1}}\right)\right) + \Psi\left(1\right) - \Psi\left(1-q\right)\right]\right\}, \end{aligned} \tag{13}$$

where q is the fractional order. $\Gamma(\cdot)$ and $\psi(\cdot)$ denote the gamma function and digamma function, respectively.

The standardized FFDispEn/ln(c^{m}) is used as FFDispEn.

2.5. Feature extraction

To measure the algorithm sensitivity to follow the complexity change in simulated signals generated by the 1D logistic map, DispEn and FFDispEn were used to extract the complexity features from the simulated signals with a sliding window of 1024 data points and an overlapping window of 64 data points. The algorithm flow is shown in Figure 3.

Furthermore, SampEn, DispEn and FFDispEn were extracted from the processed sEMG signals of the biceps brachii muscle with a sliding window of 2048 data points and an overlapping window of 256 data points so as to measure the complexity of sEMG signal under different muscle states and to detect muscle fatigue. A sliding window of 1024 data points and an overlapping window of 64 data points was also adopted for sEMG signal processing to test the data length dependence of algorithms. The algorithm flow is shown in Figure 3 as well. Curves were fit with entropy values, then the sensitivity of different algorithms to dynamic changes was tested according to the fitting characteristics. In this study, the slope of the curve and determination coefficient (R^2) were used to test the sensitivity and the anti-disturbance ability.

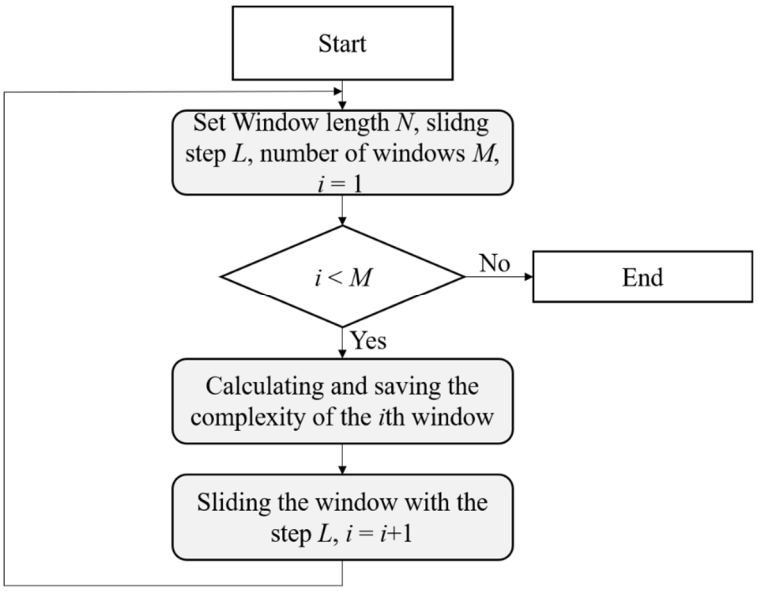

Figure 3. Flow diagram of the sliding window method.

3. Results

3.1. 1D logistic map and results

In this study, simulated signals generated by the 1D logistic map were used to study the influence of fractional order q on the entropy value [55]. The logistic map can be expressed as follows:

$$x_{i+1} = ax_i\left(1 - x_i\right), \tag{14}$$

where $0 < x_0 < 1$ and $0 < a \leq 4$. It is well known that for values of $a > 3.56995$, the 1D logistic map exhibits chaotic behavior.

In this study, parameter x_0 was set from 0.2 to 0.5 with a step size of 0.1, and parameter q was set

from −0.5 to 0.5 with a step size of 0.05 to verify the sensitivity of FFDispEn to the dynamic changes with different values of fractional order q.

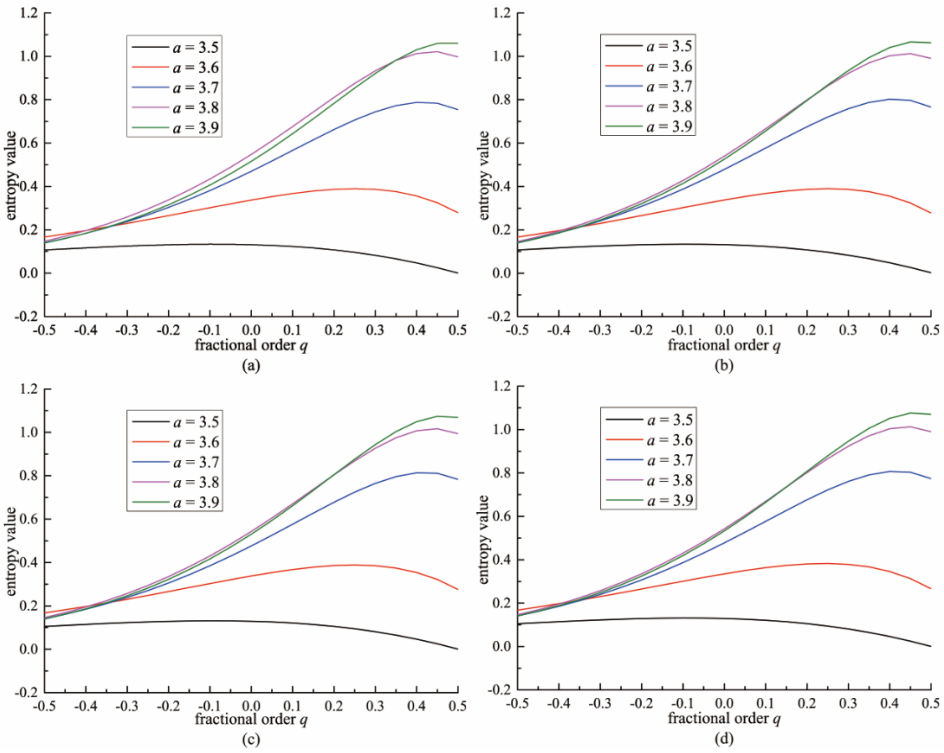

Figure 4. Mean FFDispEn value of different mapping approaches at different fractional order q. (a) $x_0 = 0.2$; (b) $x_0 = 0.3$; (c) $x_0 = 0.4$; (d) $x_0 = 0.5$.

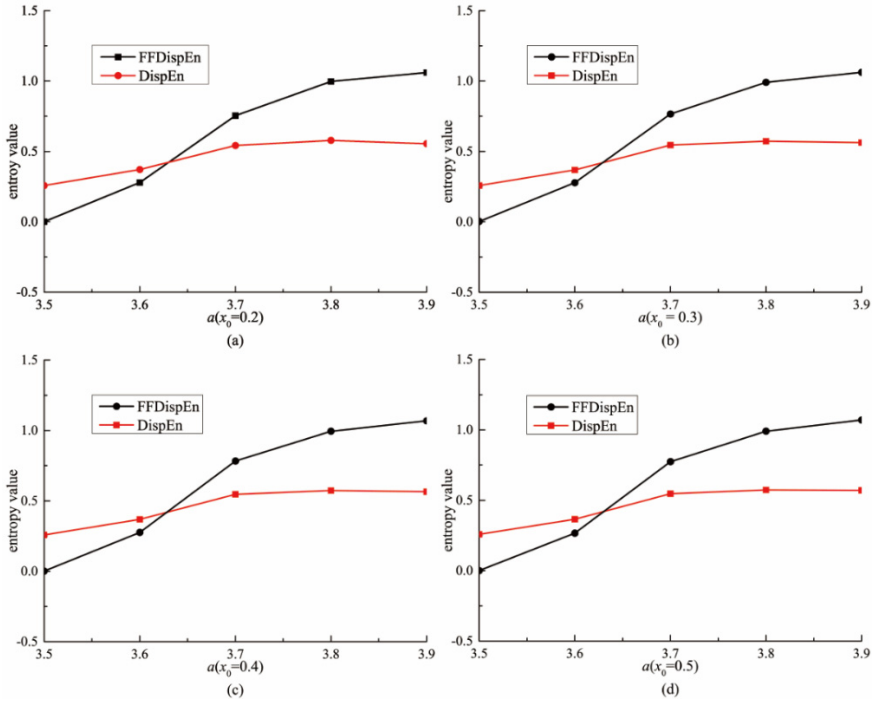

Figure 5. Mean FFDispEn and DispEn entropy values of systems of different complexities.

It can be observed from Figure 4 that the difference in entropy value between signals of different complexities increases as q increases. In particular, the discrimination performance between systems with different complexities becomes significantly better with a larger q when parameter a is 3.8 or 3.9. In conclusion, the experimental results show that the higher the fractional order of FFDispEn, the better its performance in detecting dynamic changes and in simulated signal feature extraction. As shown in formula (13), the FFDispEn becomes fuzzy DispEn when parameter q is zero. Hence, it can be concluded that FFDispEn performs better than fuzzy DispEn in detecting dynamic changes.

Moreover, it can be directly observed from Figure 5 that FFDispEn performs better than DispEn in distinguishing chaotic systems of different complexities, which means that the proposed FFDispEn is more sensitive to dynamic changes than DispEn and, thus, may perform better in muscle fatigue detection.

3.2. Muscle fatigue detection results

Curve fitting was carried out on the complexity of each frame of an sEMG signal to verify the performance of the proposed method in muscle fatigue detection. The curve fitting parameters, slope and R^2 were calculated separately to analyze the muscle fatigue process for each subject.

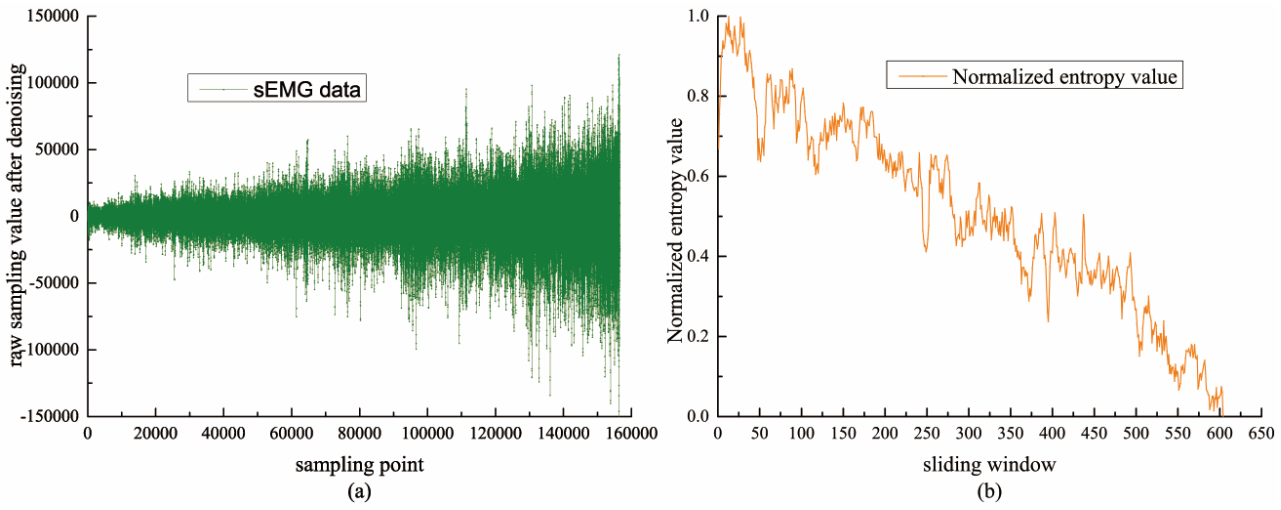

Figure 6. Muscle fatigue detection results for subject 1. (a) De-noised sEMG signal. (b) FFDispEn extracted from the preprocessed sEMG signal.

Figure 6(a) shows the de-noised sEMG signal of subject 1. Figure 6(b) shows the normalized results of FFDispEn of each frame. As can be seen, FFDispEn decreases gradually as muscle fatigue progresses, and we can then describe the fatigue process precisely. To verify the ability of the proposed algorithm to detect muscle fatigue furtherly, we fit a curve to the entropy values in Figure 6(b). The R^2 and slope were selected to verify the performance of the algorithm [23,56]. The slope reflects the algorithm's ability to follow muscle fatigue. The larger the absolute value of the slope, the stronger the ability of the algorithm to detect muscle fatigue. The R^2 reflects the anti-interference capability of the algorithm. The larger the determination coefficient, the stronger the capability of resisting interference.

In addition, the contraction duration (CD) of each subject was also calculated to reflect the fatigue

process. The results are summarized in Table 1. It can be concluded that FFDispEn performs optimally among the three algorithms in terms of the average slope value (-1.6528×10^{-3}).

Table 1 Muscle fatigue detection results of FFDispEn, DispEn and SampEn for each subject.

Subject	Slope ($\times 10^{-3}$)			R^2			CD(s)
	FFDispEn	DispEn	SampEn	FFDispEn	DispEn	SampEn	
1	−2.758	−0.234	−0.6455	0.9382	0.9431	0.9182	156
2	−3.055	−0.2441	−0.7484	0.7474	0.6869	0.5415	96.3
3	−1.351	−0.1151	−0.2982	0.8688	0.8296	0.682	319.9
4	−4.013	−0.3701	−0.8801	0.7805	0.7943	0.6798	130.7
5	−0.8891	−0.0718	−0.2346	0.671	0.6872	0.5809	203
6	−1.403	−0.1076	−0.3425	0.6500	0.6386	0.4731	138
7	−0.6104	−0.0542	−0.1876	0.4844	0.5589	0.5270	178
8	−0.5839	−0.0476	−0.2221	0.5208	0.5817	0.6186	215.4
9	−0.6643	−0.0646	−0.2762	0.7303	0.7744	0.7889	239.8
10	−2.489	−0.1828	−0.7346	0.8693	0.8427	0.8515	178.5
11	−1.198	−0.9471	−0.2473	0.4908	0.4899	0.3717	297.2
12	−0.94	−0.0872	−0.2731	0.8580	0.8964	0.8917	311
13	−1.733	−0.1463	−0.4287	0.9006	0.9220	0.8878	226.4
14	−1.315	−0.1154	−0.3148	0.8024	0.7937	0.7351	191.7
15	−1.339	−0.1068	−0.3024	0.7574	0.7576	0.6682	169.4
16	−2.127	−0.1786	−0.4677	0.7992	0.8311	0.7152	180.6
17	−1.325	−0.1029	−0.3388	0.8925	0.8862	0.8168	318.8
18	−2.769	−0.2566	−0.4718	0.8151	0.771	0.5062	97.6
19	−1.96	−0.1491	−0.5653	0.8735	0.8491	0.8615	192
20	−0.129	−0.0171	−0.0563	0.4412	0.4361	0.4014	230.6
21	−2.495	−0.1842	−0.6418	0.8837	0.8830	0.7947	187.1
22	−0.8824	−0.0698	−0.3578	0.7532	0.6965	0.8130	230
23	−1.757	−0.1407	−0.4327	0.9091	0.8987	0.8630	266.7
24	−1.219	−0.1071	−0.2706	0.8918	0.8971	0.8180	259.4
25	−1.71	−0.1292	−0.4892	0.8648	0.8817	0.8327	280.8
26	−2.798	−0.2517	−0.708	0.7465	0.7686	0.7335	160.4
27	−1.835	−0.139	−0.4383	0.5694	0.5885	0.4771	149.2
28	−1.038	−0.087	−0.3025	0.4844	0.5469	0.5633	150.2
29	−1.545	−0.1505	−0.3752	0.7567	0.8148	0.6758	151
mean	**−1.6528**	−0.1675	−0.4156	0.7500	**0.7568**	0.6927	203.7
std	0.8624	0.1652	0.1911	0.1469	0.1373	0.1558	62.1

However, FFDispEn's anti-disturbance ability is not the best among the three algorithms in terms of the mean values of R^2. The reason for this may be that we set the parameter q as 0.5 in this study, and this may lead to a high sensitivity to interference.

To further verify the effectiveness of the proposed algorithm, a two independent-sample t-test was performed to determine whether there is statistical evidence that the associated population means of different algorithms for the whole subjects group are significantly different. The statistical results are

shown in Table 2. Compared with DispEn and SampEn, the absolute value of the slope for FFDispEn increased significantly, as seen in Table 2. There is statistic difference between the three entropy metrices ($P < 0.05$). Meanwhile, DispEn performed worst in muscle fatigue detection (with a mean slope of -1.675×10^{-4}). These results indicate that FFDispEn is more sensitive to dynamic change and can reflect muscle fatigue more precisely, accurately and stably compared to other algorithms.

Table 2. Two independent-sample t-test for fatigue detection and algorithm.

	Mean			
	FFDispEn	DispEn	SampEn	$P < 0.05$
slope	-1.6528×10^{-3}	-1.675×10^{-4}	-4.156×10^{-4}	

3.3. Muscle fatigue classification with SVM

To further evaluate the discriminative ability of FFDispEn, DispEn and SampEn to distinguish muscle non-fatigue and fatigue states, the experimental data of the 29 subjects was divided into a training dataset (80%) and a test dataset (20%). SVM classifier with the radial basis function (RBF) kernel function was employed for non-fatigue and fatigue classification. In order to reflect the performance of the algorithm more accurately, only the entropy-based features were used to classify the muscle states. A K-fold cross-validation approach with K = 5 was employed to determine the optimal classification model. Accuracy, sensitivity, specificity, precision, F1-score and receiver operating characteristic (ROC) curves [44,46] were used to evaluate the models' ability to identify fatigued states. The expression of performance metrics is given as follows.

$$\text{Accuracy} = \frac{TP + TN}{TP + TN + FP + FN} \tag{15}$$

$$\text{Sensitivity} = \frac{TP}{TP + FN} \tag{16}$$

$$\text{Specificity} = \frac{TN}{FP + TN} \tag{17}$$

$$\text{Precision} = \frac{TP}{TP + FP} \tag{18}$$

$$\text{F1-score} = \frac{2TP}{2TP + FP + FN} \tag{19}$$

Here, *TP*, *TN*, *FP* and *FN* are true positive, true negative, false positive and false negative, respectively.

The results are shown in Tables 3 and 4 and Figures 7–10. As we can see from Tables 3 and 4, a highest accuracy of 97.5% is achieved based on the FFDispEn and SVM in classifying non-fatigue and fatigue conditions with a sliding windows length of 2048 data points, and an accuracy of 95% was achieved with a sliding windows length of 1024 data points. The sensitivity, specificity, precision and F1-score were also found to be greater compared with other classifiers. These results further confirm the effectiveness of the proposed algorithm.

Table 3 Comparison of the classification results (in %) of different feature types by SVM classification algorithms (sliding windows length = 1024 data points).

Feature	Classifier	Sensitivity	Specificity	Precision	F1-score	Accuracy
FFDispEn	SVM	90	100	100	94.74	95
DispEn	SVM	90	95	94.74	92.31	92.5
SampEn	SVM	95	85	86.36	90.48	90

Table 4 Comparison of the classification result (in %) of different feature types by SVM classification algorithms (sliding windows length = 2048 data points).

Feature	Classifier	Sensitivity	Specificity	Precision	F1-score	Accuracy
FFDispEn	SVM	100	95	95.24	97.56	97.5
DispEn	SVM	95	95	95	95	95
SampEn	SVM	90	95	94.74	92.31	92.5

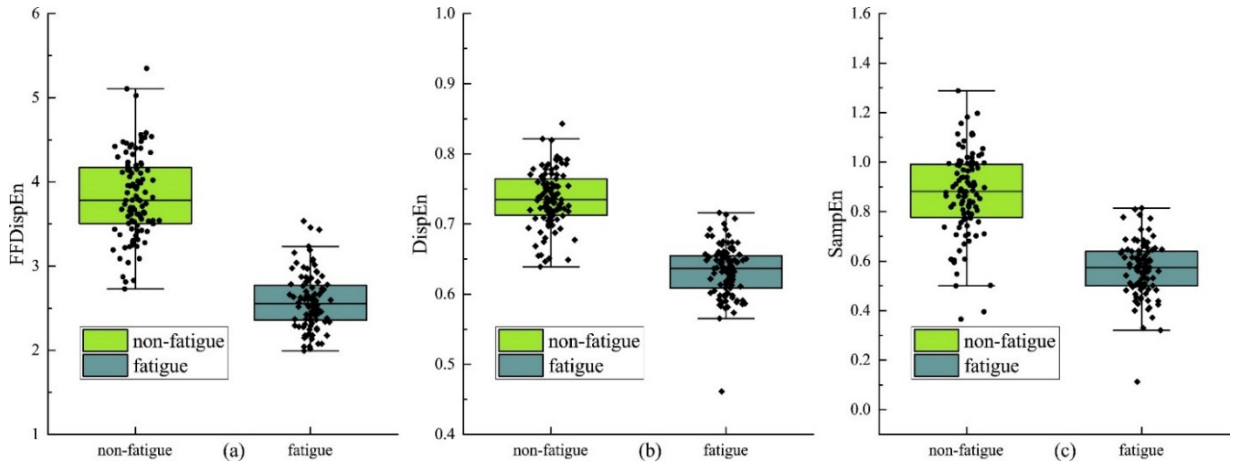

Figure 7. Mean values of (a) FFDispEn, (b) DispEn, (c) SampEn in state of Non-fatigue/Fatigue with a sliding window length of 1024 data points.

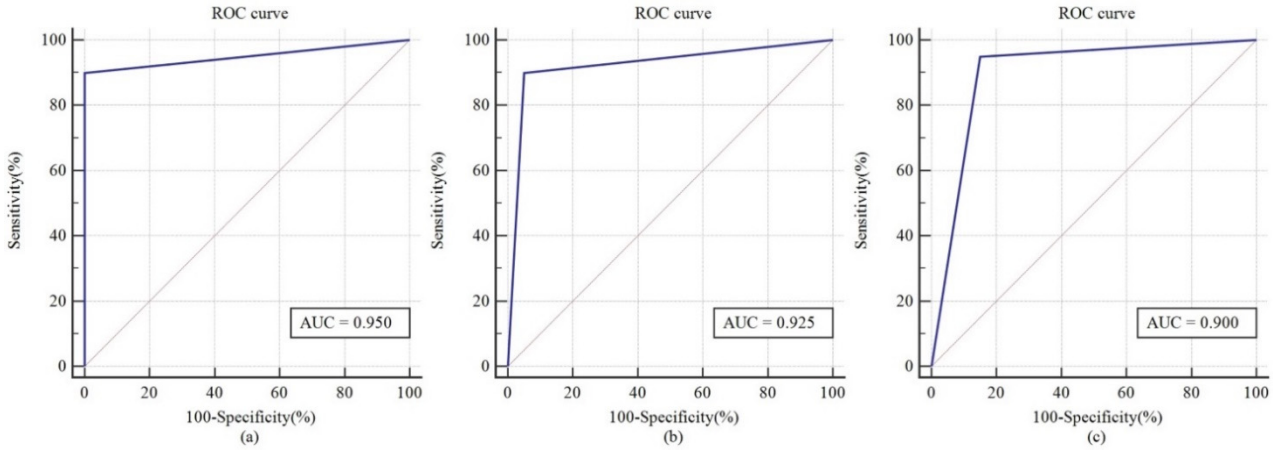

Figure 8. Non-fatigue/Fatigue classification using (a) FFDispEn and SVM (b) DispEn and SVM (c) SampEn and SVM, with a sliding window length of 1024 data points.

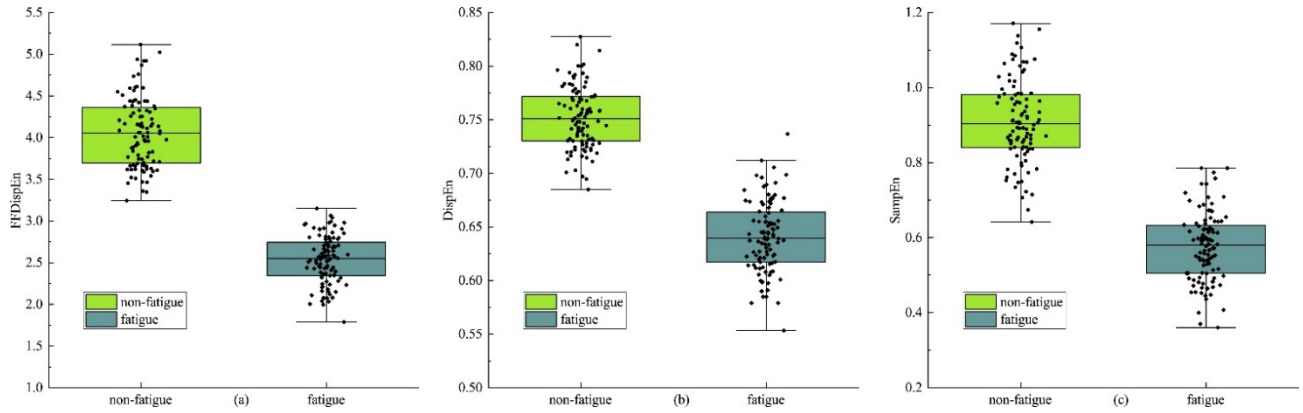

Figure 9. Mean values of (a) FFDispEn, (b) DispEn, (c) SampEn in state of Non-fatigue/Fatigue with a sliding window length of 2048 data points.

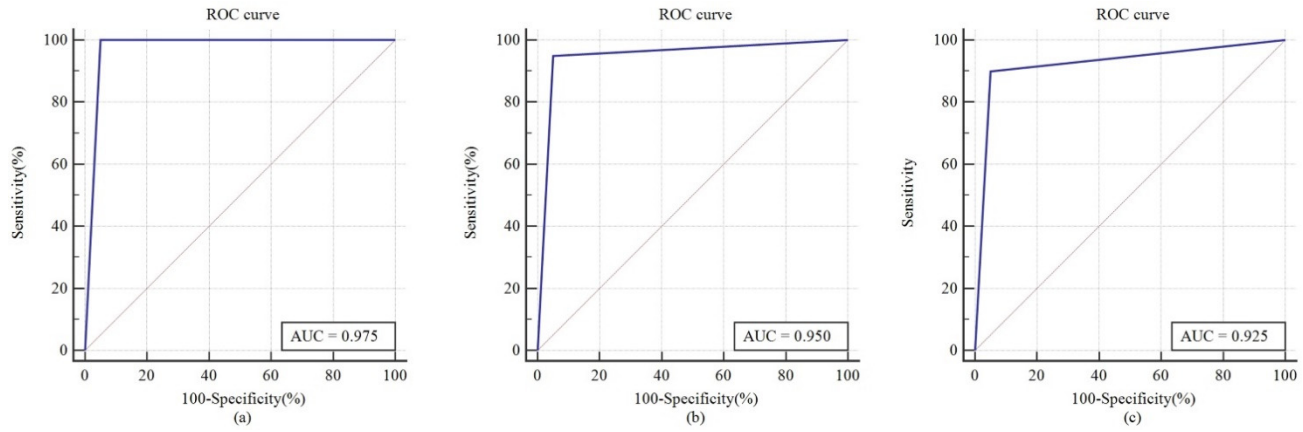

Figure 10. Non-fatigue/Fatigue classification using (a) FFDispEn and SVM (b) DispEn and SVM (c) SampEn and SVM, with a sliding window length of 2048 data points.

Figures 7 and 8 showed the results of using the SVM algorithm to identify muscle fatigue based on the entropy features with a sliding window length of 1,024 data points. The results showed that the recognition accuracy of identification framework based on FFDispEn and SVM is 95% with an area under the ROC curve (AUC) of 0.95, while the recognition accuracy of identification framework based on DispEn and SVM is 92.5% with an AUC of 0.925. Furthermore, the SampEn and SVM recognition accuracy is 90% with an AUC of 0.90.

Figures 9 and 10 showed the results of using the SVM algorithm to identify muscle fatigue based on the entropy features with a sliding window length of 2,048 data points. The results show that the recognition accuracy of identification framework based on FFDispEn and SVM is 97.5% with an AUC of 0.975, while the recognition accuracy of identification framework based on DispEn and SVM is 95% with an AUC of 0.95. Furthermore, the SampEn and SVM recognition accuracy is 92.5% with an AUC of 0.925. These results indicated that FFDispEn has a clear decreasing trend as muscle fatigue processes and is more sensitive to dynamic changes compared to SampEn and DispEn. The proposed framework with FFDispEn and the SVM classifier is suitable for muscle fatigue detection.

4. Discussion

4.1. FFDispEn

Entropy is an important metric used to measure signal complexity. In recent years, various entropy-based measurement methods have been used to quantify the complexity of different types of complicated, nonstationary, nonlinear signals. In this study, a new method called FFDispEn is proposed based on DispEn, a fuzzy membership function and fractional calculus. From the above analysis, it can be concluded that FFDispEn performs better than SampEn and DispEn in muscle fatigue detection and simulation signal analysis. Hence, we provide a new method for the measurement of signal complexity in the biomedical engineering field.

Compared with SampEn and fuzzy entropy, DispEn has the advantage of having lower sensitivity to noise and data length. When analyzing time series with a smaller data length, there will be no undefined entropy value in DispEn, and the calculation of entropy takes into account important information: Time series amplitude. It can detect changes in amplitude and frequency at the same time. Moreover, the calculation speed of DispEn is fast. This characteristic makes it easy to apply DispEn in real-time applications [9]. However, DispEn is still sensitive to parameter selection and signal length as well as SampEn to some extent. In addition, small changes in the amplitude of the time series due to noise can also change the entropy value dramatically [9].

Rostaghi et al. [17] proposed fuzzy DispEn for the first time and verified its advantages over DispEn. Furthermore, Li proposed fractional order fuzzy DispEn based on fractional calculus and verified its advantage in signal complexity analysis [57]. In this study, a novel fuzzy membership function based on Euclidean distance is proposed. Euclidean distance can reflect the relationship between two sequences more precisely and fully. Thus, the novel fuzzy membership function can lead to a smaller loss in signal information during its mapping to its dispersion patterns. Additionally, compared with these works, one of the strengths of the present study is that we propose a fuzzy membership function based on Euclidean distance and an adjustable threshold parameter r. During entropy calculation, the Euclidean distances between the embedding vectors and dispersion patterns are first calculated, then the dispersion pattern whose Euclidean distance is less than the set threshold r is selected. The probability of the occurrence of the corresponding dispersion pattern is allocated according to the size of Euclidean distance. In actual applications, we can set different thresholds r to meet different usage requirements. Despite the above advantages, fuzzy DispEn, which combines fuzzy membership function and DispEn, suffers from limitation of insensitivity to dynamic changes. Hence, fractional calculus is proposed to increase sensitivity to dynamic changes to solve this problem in this study. In conclusion, our experimental results show that the proposed method has certain advantages compared to DispEn and SampEn. FFDispEn performs better than SampEn and DispEn in simulation signal analysis and muscle fatigue detection.

However, there still exists some disadvantages of the proposed method. One of the drawbacks is the increasing computational complexity caused by the fuzzy membership function. Thus, this will lead to a poor real-time performance, especially when processing long time series. As mentioned before, SCDE is also proposed to improve sensitivity to dynamic changes, and results showed it performed better in detecting various changes in time series [18]. Moreover, SCDE can also reduce the computational consumption while ensuring the accuracy and sensitivity of complexity calculation [18]. Wang et al. also proposed a rapid refined composite multiscale sample entropy [23].

These methods provide us with new ways to improve the sensitivity of dynamic change and reduce computational complexity as well. Another drawback of this study is that the optimal parameter in muscle fatigue detection is manually set based on experience. Further research is still needed on how different threshold r, fractional order parameter q and sliding window length settings affect the results. Finally, the muscle fatigue experiment paradigm needs to be further standardized. It should be noted that there are many other advanced and improved entropy-based algorithms, such as hierarchical dispersion entropy [58] and adaptive hierarchical entropy [59]. Therefore, in future work, our proposed algorithm will be modified by introducing the advantages of these advanced algorithms in order to obtain more accurate measurements of complexity and increased sensitivity to dynamic changes.

4.2. Muscle fatigue detection

Muscle fatigue can reduce the accuracy, efficiency and stability of work and rehabilitation training and, hence, can increase the risk of neuromuscular disorders. Therefore, a precise and stable method to detect muscle fatigue has important significance in healthcare and rehabilitation fields. The sEMG signal is commonly used to study muscle fatigue. Studies have pointed out that the complexity analysis of sEMG signals is a powerful tool to detect muscle fatigue [35].

In this study, FFDispEn is proposed for muscle fatigue detection. To this end, sEMG signals of subjects' biceps brachii muscles were collected. Experimental results indicated that FFDispEn can detect muscle fatigue precisely and stably. However, this study only conducted static muscle contraction fatigue detection experiments with healthy subjects. The next step is to verify the performance of the proposed method in stroke patients undergoing rehabilitation training.

4.3. Clinical implications

Signal complexity analysis has been widely used in biomedical engineering and clinical fields. On the one hand, most of the biomedical signals, such as electroencephalogram (EEG) and sEMG signals, are non-stationary, complex and nonlinear [44]. From the perspective of mathematical analysis, entropy metric is effective in biomedical signal processing and is a powerful tool in detecting dynamic changes of these signals [14,15]. On the other hand, numerous studies have confirmed that entropy-based complexity metrics can effectively measure the patients' status and assist in the diagnostic process [45]. In view of this, FFDispEn can provide a better entropy-based complexity metric for clinical applications, such as rehabilitation evaluation and automated diagnosis of Parkinson's disease, due to its high sensitivity to dynamic changes.

In this study, FFDispEn has been used in muscle fatigue detection, and results showed that FFDispEn can detect muscle fatigue more precisely and effectively compared to other entropy-based detection methods. The urgent willingness for rehabilitation and subjective perception delay of muscle endurance of stroke patients can result in incidences of secondary injury in clinic. Muscle fatigue state can be detected with FFDispEn more accurately to avoid secondary injuries and ensure the safety of rehabilitation training. In addition, the real-time muscle fatigue monitoring can be realized through combination of SVM and FFDispEn.

Finally, the framework proposed in this study can also be applied in other data processing fields. In future studies, we will further explore the application of the proposed method in other clinical areas, such as medical image and EEG signal processing. Studies on different types of patients, such as

epileptic and stroke patients, will be conducted with multiple trials to further translate the proposed framework approach to clinical fields.

4.4. Limitations of this study and future work

First, only 29 subjects were recruited for muscle fatigue detection in this study. It is essential to increase the number of participants to demonstrate the effectiveness of the proposed algorithm in detecting dynamic changes in future work. Second, the experiment's procedure only involves muscle fatigue detection with a specific load during static muscle contractions. Studying the muscle fatigue progress during dynamic contractions is necessary. How different weight-bearing tasks affect muscle fatigue also requires further investigation. Moreover, FFDispEn's application to stroke patients in clinical environments requires testing and validation.

Parameter q is a key parameter in FFDispEn. In this study, results with q set from −0.5 to 0.5 was analyzed to find out the optimal parameter setting. FFDispEn with $q_{\max}$ obtains the best results for simulated signals generated by the 1D logistic map, where $q_{\max}$ is 0.5 in this study. It can be concluded that FFDispEn is effective in analyzing chaotic systems and that $q_{\max}$ is a good choice when we want to detect dynamic changes. Thus, the optimal parameter was also set as $q_{\max}$ experientially in muscle fatigue detection. Results demonstrated that FFDispEn with $q_{\max}$ performed better than DispEn and SampEn in muscle fatigue detection as well. However, the absolute value of the slope of FFDispEn may increase with the increase in fractional order after a certain value of q to some subjects in muscle fatigue analysis. Therefore, $q_{\max}$ may not always be the best parameter to employ in muscle fatigue detection experiment. The reason for this may be that subjects involuntarily adjust their muscle state while maintaining the static posture. FFDispEn is sensitive to dynamic changes and a bigger q corresponds to a higher sensitivity to such changes. Hence, parameter q may result in large complexity changes even with small muscle state changes.

We can also draw this conclusion from Table 1. As seen from Table 1, FFDispEn's anti-disturbance ability is not the best among the three algorithms. The reason for this may be that we set the parameter q as 0.5 in this study, and this may lead to a high sensitivity to interference. To further determine the optimal parameters, the follow-up research plan is to optimize the static muscle contraction experiment and to test different parameter combinations. Moreover, we will design dynamic muscle contraction experiments to test the sensitivity of FFDispEn to dynamic changes as muscle fatigue progresses so as to minimize the involuntary muscle regulation during the experiment. In addition, we simply set m to three and c to seven in this study. Optimizing these parameters combination also requires attention.

Finally, we only compared the performance of the proposed FFDispEn with that of DispEn and SampEn, but not with that of fuzzy DispEn. The fuzzy membership function proposed in this study is based on Euclidean distance, which is different from the fuzzy membership function proposed in the literature [17]. Since the Euclidean distance can reflect the distance of the two subsequences fully [60], our proposed algorithm may better measure signal complexity than fuzzy DispEn [17], but a proper comparison should be made in future work. Furthermore, the new method proposed in this study, which combines fuzzy membership function and fractional calculus, may also be used in medical image and EEG signal processing and analysis, such as biomedical image segmentation and disease diagnosis [43,45,61]. We will further expand the application of the method in future research.

Table 5 summarizes the methods, classifier and accuracy of some contemporary works related to

muscle fatigue detection. As can be seen from the table, signal analysis methods in time domain, frequency domain, time-frequency domain and nonlinear domain, such as S-transform, VMD and entropy-based complexity metrics, have been proposed for sEMG signal features extraction in muscle fatigue detection.

Table 5 Comparison with literature.

Reference	Methods and features	Classifier	Accuracy (%)
[62]	two time-domain features and two frequency domain features	Double-Step Binary Classifier	94.46
[40]	S-transform, B-distribution	SVM	91.39
[38]	PE	LR	80
[63]	Fourier accumulation method, Geometric features	ELM and MLP	94
[64]	Weighted Visibility Graph Features	ELM	89.1
[65]	VMD and Hjorth features	random forest	92.2
[66]	Combined fuzzy recurrence networks feature	KNN	96.90
[67]	bubble entropy	KNN	87.5
[46]	maximum effective degrees	Thresholds estimated with ROC	90.38
[68]	the electrodermal activity and heart rate variability series	SVM	83.33
[69]	multi-information fusion method	SVM	97 ± 0.28
[39]	major axis length, area, perimeter, second order moment and central moment	MLP	86
[70]	CNN and three types of commonly used statistical algorithms	SVM	96.5
[71]	multi-modal feature information fusion, component analysis, grey relational analysis	Extreme gradient boosting, SVM	89.47
[72]	multi-feature information fusion	SVM, RF	85-90
[73]	features in time-domain, frequency-domain, time-frequency domain, and nonlinear domain	SVM With Improved Whale Optimization Algorithm	85.5
[74]	approximate entropy and permutation entropy, deep learning	CNN-LSTM Transformer	96.67
[75]	one-dimensional feature and two-dimensional feature extraction	LSTM	99.4
[76]	fuse features of time domain and frequency domain	Multi-dimensional Feature Fusion Network	96.45/78.25
[77]	sEMG signals and deep learning	Attention-LSTM	93.5
[42]	two time-domain features and two frequency domain features	LSTM	95.18
[41]	time-domain features, frequency domain features and entropy-based features	CNN–SVM	86.69
Our Work	FFDispEn	SVM	97.5

Sasidharan et al. used Hjorth parameters, bubble entropy and the machine learning algorithm to detect muscle fatigue states, achieving a highest accuracy of 95% [67]. These methods are based on traditional machine learning and manually extracted features from sEMG signals [38–40,67]. However, biomedical signals are non-stationary, complex and nonlinear [23,30,45]. Therefore, it is challenging to analyze such complex signals and to extract features for traditional machine learning algorithms. Deep learning algorithms can automatically extract important classification features from raw data and show more efficient and accurate results in large datasets [44]. Recently, deep learning has been increasingly used in biomedical signal processing and has outperformed traditional machine learning methods [44]. Dang et al. proposed a fatigue assessment method based on three deep learning algorithms and obtained 93.5% assessment accuracy using attention-LSTM [77]. However, a deep learning approach requires more computational resources and precise selection of hyperparameters, which is a comparatively difficult task compared to traditional machine learning [45]. Compared with these methods, our method achieved a highest accuracy of 97.5% in isometric muscle fatigue detection using the SVM classifier. It should be noted that our method only uses entropy-based features to classify muscle fatigue states during static contractions. However, simple experiment design and insufficient data may also lead to these results. Moreover, the contraction duration of each subject is quite different. The effect of the difference on muscle fatigue also needs to be studied. Thus, a lot of research still needs to be conducted before practical application. In summary, the proposed framework with FFDispEn and the SVM classifier may be suitable for real-time muscle fatigue state monitoring.

5. Conclusions

Based on a fuzzy membership function and fractional calculus, FFDispEn was proposed and applied to muscle fatigue detection in this study. First, the 1D logistic map generated chaotic sequences to test the algorithm's sensitivity to dynamic changes. The results show that the sensitivity of FFDispEn to dynamic change increases with increasing fractional parameter q; additionally, FFDispEn performs better than DispEn in following complexity changes. A muscle fatigue experiment was performed on 29 subjects with the sEMG signals of biceps brachii being recorded. Compared with DispEn and SampEn, FFDispEn showed better performance in muscle fatigue detection. Moreover, results showed that FFDispEn can describe the fatigue process of most subjects more precisely, accurately and stably. The highest accuracy of 97.5% was achieved with the FFDispEn and SVM. The muscle fatigue detection results and comparison with contemporary research have demonstrated that the FFDispEn and a SVM classifier is a promising approach for muscle fatigue detection and monitoring. These results demonstrate that the proposed algorithm is more sensitive to dynamic changes. We hope that this new nonlinear method will also show good performance in diagnostic applications, such as stroke patients' muscle fatigue detection and epilepsy prediction in a clinical environment.

Use of AI tools declaration

The authors declare they have not used Artificial Intelligence (AI) tools in the creation of this article.

Acknowledgments

This work was supported in part by Key Project of Natural Science Research of Universities in Anhui Province (2022AH051804), in part by Talent Research Fund of Hefei University (21-22RC01) and in part by the National Natural Science Foundation of China under Grant No. U1713210.

Conflict of interest

The authors declare there is no conflict of interest.

References

1. V. Khodadadi, F. N. Rahatabad, A. Sheikhani, N. J. Dabanloo, Nonlinear analysis of biceps surface EMG signals for chaotic approaches, *Chaos Soliton Fract.*, **166** (2023), 112965. https://doi.org/10.1016/j.chaos.2022.112965
2. X. Zhang, P. Zhou, Sample entropy analysis of surface EMG for improved muscle activity onset detection against spurious background spikes, *J. Electromyogr. Kinesiology,* **22** (2012), 901–907. https://doi.org/10.1016/j.jelekin.2012.06.005
3. Z. Brari, S. Belghith, A new algorithm for largest Lyapunov exponent determination for noisy chaotic signal studies with application to Electroencephalographic signals analysis for epilepsy and epileptic seizures detection, *Chaos Soliton Fract.*, **165** (2022), 112757. https://doi.org/10.1016/j.chaos.2022.112757
4. S. B. He, K. H. Sun, R. X. Wang, Fractional fuzzy entropy algorithm and the complexity analysis for nonlinear time series, *Eur. Phys. J. Special Topics*, **227** (2018), 943–957. https://doi.org/10.1140/epjst/e2018-700098-x
5. K. Harezlak, P. Kasprowski, Application of time-scale decomposition of entropy for eye movement analysis, *Entropy*, **22** (2020), 68. https://doi.org/10.3390/e22020168
6. S. Jia, B. Ma, W. Guo, Z. S. Li, A sample entropy based prognostics method for lithiumion batteries using relevance vector machine, *J. Manuf. Sys.*, **61** (2021), 773–781. https://doi.org/10.1016/j.jmsy.2021.03.019
7. J. Richman, J. Moorman, Physiological time-series analysis using approximate entropy and sample entropy, *Am. J. Physiol. Heart Circ. Physiol*., **278** (2000), H2039–H2049. https://doi.org/10.1152/ajpheart.2000.278.6.H2039
8. W. T. Chen, Z. Z. Wang, H. B. Xie, W. X. Yu, Characterization of surface EMG signal based on fuzzy entropy, *IEEE Trans. Neural Syst. Rehabil. Eng*., **15** (2007), 266–272. https://doi.org/10.1109/TNSRE.2007.897025
9. M. Rostaghi, H. Azami, Dispersion Entropy: A measure for time-series analysis, *IEEE Signal Proc. Let*., **23** (2016), 610–614. https://doi.org/10.1109/LSP.2016.2542881
10. S. B. Jiao, B. Geng, Y. X. Li, Q. Zhang, Q. Wang, Fluctuation-based reverse dispersion entropy and its applications to signal classification, *Appl. Acoust*., **175** (2021), 107857. https://doi.org/10.1016/j.apacoust.2020.107857
11. H. Azami, M. Rostaghi, D. Abásolo, J. Escudero, Refined composite multiscale dispersion entropy and its application to biomedical signals, *IEEE Trans. Bio-med. Eng*., **64** (2017), 2872–2879. https://doi.org/10.1109/TBME.2017.2679136

12. S. Sharma, S. K. Tiwari, A novel feature extraction method based on weighted multi-scale fluctuation based dispersion entropy and its application to the condition monitoring of rotary machines, *Mech. Syst. Signal Pr.*, **171** (2022), 108909. https://doi.org/10.1016/j.ymssp.2022.108909
13. C. J. Li, Y. C. Wu, H. J. Lin, J. M. Li, F. Zhang, Y. X. Yang, ECG denoising method based on an improved VMD algorithm, *IEEE Sens J.*, **22** (2022), 22725–22733. https://doi.org/10.1109/JSEN.2022.3214239
14. B. García-Martínez, A. Fernández-Caballero, R. Alcaraz, A. Martínez-Rodrigo, Application of dispersion entropy for the detection of emotions with electroencephalographic signals, *IEEE T. Cogn. Dev. Syst*., **14** (2022), 1179–1187. https://doi.org/10.1109/TCDS.2021.3099344
15. E. Kafantaris, T. Y. M. Lo, J. Escudero, Stratified multivariate multiscale dispersion entropy for physiological signal analysis, *IEEE Trans. Bio-med Eng.*, **70** (2023), 1024–1035. https://doi.org/10.1109/TBME.2022.3207582
16. Q. F. Wang, Y. Xiao, S. Wang, W. C. Liu, X. J. Liu, A method for constructing automatic rolling bearing fault identification model based on refined composite multi-scale dispersion entropy, *IEEE Access*, **9** (2021), 86412–86428. https://doi.org/10.1109/ACCESS.2021.3089251
17. M. Rostaghi, M. M. Khatibi, M. R. Ashory, H. Azami, Fuzzy dispersion entropy: A nonlinear measure for signal analysis, *IEEE Trans. Fuzzy Syst.*, **30** (2021), 3785–3796. https://doi.org/10.1109/TFUZZ.2021.3128957
18. Y. X. Li, B. Geng, B. Z. Tang, Simplified coded dispersion entropy: A nonlinear metric for signal analysis, *Nonlinear Dyn*., **111** (2023), 9327–9344. https://doi.org/10.1007/s11071-023-08339-4
19. J. P. Ugarte, J. A. Tenreiro Machado, C. Tobón, Fractional generalization of entropy improves the characterization of rotors in simulated atrial fibrillation, *Appl. Math. Comput*., **425** (2022), 127077. https://doi.org/10.1016/j.amc.2022.127077
20. A. D. Crescenzo, S. Kayal, A. Meoli, Fractional generalized cumulative entropy and its dynamic version, *Commun. Nonlinear Sci*., **102** (2021), 105899. https://doi.org/10.1016/j.cnsns.2021.105899
21. Y. Wang, P. J. Shang, Complexity analysis of time series based on generalized fractional order cumulative residual distribution entropy, *Phys. A*, **537** (2020), 122582. https://doi.org/10.1016/j.physa.2019.122582
22. J. T. Machado, Fractional order generalized information, *Entropy*, **16** (2014), 2350–2361. https://doi.org/10.3390/e16042350
23. S. R. Wang, H. Tang, B. Wang, J. Mo, Analysis of fatigue in the biceps brachii by using rapid refined composite multiscale sample entropy, *Biomed. Signal Process*., **67** (2021), 102510. https://doi.org/10.1016/j.bspc.2021.102510
24. I. Yun, J. Jeung, Y. Song, Y. Chung, Non-Invasive quantitative muscle fatigue estimation based on correlation between sEMG signal and muscle mass, *IEEE Access*, **8** (2020), 191751–191757. https://doi.org/10.1109/ACCESS.2020.3029792
25. D. R. Rogers, D. T. MacIsaac, EMG-based muscle fatigue assessment during dynamic contractions using principal component analysis, *J. Electromyogr. Kinesiology*, **21** (2011), 811–818. https://doi.org/10.1016/j.jelekin.2011.05.002
26. J. R. Mota-Carmona, F. Pérez-Escamirosa, A. Minor-Martínez, R. M. Rodríguez-Reyna, Muscle fatigue detection in upper limbs during the use of the computer mouse using discrete wavelet transform: A pilot study, *Biomed. Signal Process*., **76** (2022), 103711. https://doi.org/10.1016/j.bspc.2022.103711

27. B. K. Barry, R. M. Enoka, The neurobiology of muscle fatigue: 15 years later, *Integr. Comput. Biol*., **47** (2007), 465–473. https://doi.org/10.1093/icb/icm047
28. W. K. Xu, B. Chu, E. Rogers, Iterative learning control for robotic-assisted upper limb stroke rehabilitation in the presence of muscle fatigue, *Control Eng. Pract*., **31** (2014), 63–72. https://doi.org/10.1016/j.conengprac.2014.05.009
29. F. F. Wang, E. M. Yiu, Is surface Electromyography (sEMG) a useful tool in identifying muscle tension dysphonia? An integrative review of the current evidence, *J. Voice*, **10** (2021). https://doi.org/10.1016/j.jvoice.2021.10.006
30. J. Hussain, K. Sundaraj, F. L. Yin, L. C. Kiang, S. Sundaraj, M. A. Ali, A systematic review on fatigue analysis in triceps brachii using surface electromyography, *Biomed. Signal Process*., **40** (2018), 396–414. https://doi.org/10.1016/j.bspc.2017.10.008
31. S. E. Jero, K. D. Bharathi, P. A. Karthick, S. Ramakrishnan, Muscle fatigue analysis in isometric contractions using geometric features of surface electromyography signals, *Biomed. Signal Process*., **68** (2021), 102603. https://doi.org/10.1016/j.bspc.2021.102603
32. G. Y. Zhang, E. Morin, Y. X. Zhang, S. A. Etemad, Non-invasive detection of low-level muscle fatigue using surface EMG with wavelet decomposition, in *40th Annual International Conference of the IEEE Engineering in Medicine and Biology Society (EMBC)*, (2018), 5648–5651. https://doi.org/10.1109/EMBC.2018.8513588
33. M. Cifrek, V. Medved, S. Tonković, S. Ostojić, Surface EMG based muscle fatigue evaluation in biomechanics, *J Clin. Biomech.*, **24** (2009), 327–340. https://doi.org/10.1016/j.clinbiomech.2009.01.010
34. W. W. Hu, Y. C. Huang, C. P. Li, Improved algorithm of muscle fatigue detection using linear regression analysis, *Electron. Lett*., **49** (2013), 89–91. https://doi.org/10.1049/el.2012.2316
35. H. B. Xie, Z. Z. Wang, Mean frequency derived via Hilbert-Huang transform with application to fatigue EMG signal analysis, *Comput. Methods Prog. Biomed*., **82** (2006), 114–120. https://doi.org/10.1016/j.cmpb.2006.02.009
36. H. B. Xie, J. Y. Guo, Y. P. Zheng, Fuzzy approximate entropy analysis of chaotic and natural complex systems: detecting muscle fatigue using electromyography signals, *Ann. Biomed. Eng*., **38** (2010), 1483–1496. https://doi.org/10.1007/s10439-010-9933-5
37. A. Shoeibi, M. Khodatars, M. Jafari, N. Ghassemi, P. Moridian, R. Alizadehsani, et al., Diagnosis of brain diseases in fusion of neuroimaging modalities using deep learning: A review, *Inf. Fusion*, **93** (2023), 85–117. https://doi.org/10.1016/j.inffus.2022.12.010
38. J. Murillo-Escobar, Y. E. Jaramillo-Munera, D. A. Orrego-Metaute, E. Delgado-Trejos, D. Cuesta-Frau, Muscle fatigue analysis during dynamic contractions based on biomechanical features and Permutation Entropy, *Math. Biosci. Eng*., **17** (2020), 2592–2615. https://doi.org/10.3934/mbe.2020142
39. S. E. Jero, K. D. Bharathi, P. A. Karthick, S. Ramakrishnan, Muscle fatigue analysis in isometric contractions using geometric features of surface electromyography signals, *Biomed. Signal Process*., **68** (2021), 102603. https://doi.org/10.1016/j.bspc.2021.102603
40. P. A. Karthick, D. M. Ghosh, S. Ramakrishnan, Surface electromyography based muscle fatigue detection using high-resolution time-frequency methods and machine learning algorithms, *Comput. Methods Prog. Biomed*., **154** (2018), 45–56. https://doi.org/10.1016/j.cmpb.2017.10.024

41. J. H. Wang, Y. N. Sun, S. M. Sun. Recognition of muscle fatigue status based on improved wavelet threshold and CNN-SVM, *IEEE Access*, **8** (2020), 207914–207922. https://doi.org/10.1109/ACCESS.2020.3038422
42. J. H. Wang, S. M. Sun, Y. N. Sun, A muscle fatigue classification model based on LSTM and improved wavelet packet threshold, *Sensors*, **21** (2021), 6369. https://doi.org/10.3390/s21196369
43. A. Shoeibi, M. Rezaei, N. Ghassemi, Z. Namadchian, A. Zare, J. M. Gorriz, Automatic diagnosis of schizophrenia in EEG signals using functional connectivity features and CNN-LSTM model, in *Proceedings of the International Work-Conference on the Interplay Between Natural and Artificial Computation (IWINAC)*, (2022), 63–73. https://doi.org/10.1007/978-3-031-06242-1_7
44. M. Jafari, D. Sadeghi, A. Shoeibi, H. Alinejad-Rokny, A. Beheshti, D. López-García, et al., Empowering precision medicine: AI-Driven schizophrenia diagnosis via EEG signals: A comprehensive review from 2002–2023, *Appl. Intell.*, **2023** (2023), 1–45. https://doi.org/10.1007/s10489-023-05155-6
45. P. Chawla, S. B. Rana, H. Kaur, K. Singh, R. Yuvaraj, M. Murugappan, A decision support system for automated diagnosis of Parkinson's disease from EEG using FAWT and entropy features, *Biomed. Signal Process*., **79** (2023), 104116. https://doi.org/10.1016/j.bspc.2022.104116
46. N. Makaram, P. A. Karthick, R. Swaminathan, Analysis of dynamics of EMG signal variations in fatiguing contractions of muscles using transition network approach, *IEEE Trans. Instrum. Meas*., **70** (2021), 4003608. https://doi.org/10.1109/TIM.2021.3063777
47. C. Tepe, M. C. Demir, Real-time classification of EMG Myo armband data using support vector machine, *IRBM*, **43** (2022), 300–308. https://doi.org/10.1016/j.irbm.2022.06.001
48. X. J. Wang, D. P. Dong, X. K. Chi, S. P. Wang, Y. N. Miao, M. L. An, et al., sEMG-based consecutive estimation of human lower limb movement by using multi-branch neural network, *Biomed. Signal Process.*, **68** (2021), 102781. https://doi.org/10.1016/j.bspc.2021.102781
49. J. R. Potvin, L. R. Bent, A validation of techniques using surface EMG signals from dynamic contractions to quantify muscle fatigue during repetitive tasks, *J. Electromyogr. Kinesiology*, **7** (1997), 131–139. https://doi.org/10.1016/S1050-6411(96)00025-9
50. K. Dragomiretskiy, D. Zosso, Variational mode decomposition, *IEEE Trans. Signal Process*., **62** (2014), 531–544. https://doi.org/10.1109/TSP.2013.2288675
51. H. Ashraf, U. Shafiq, Q. Sajjad, A. Waris, O. Gilani, M. Boutaayamou, et al., Variational mode decomposition for surface and intramuscular EMG signal denoising, *Biomed. Signal Process.*, **82** (2023), 104560. https://doi.org/10.1016/j.bspc.2022.104560
52. S. H. Ma, B. Lv, C. Lin, X. J. Sheng, X. Y. Zhu, EMG signal filtering based on variational mode decomposition and sub-band thresholding, *IEEE J. Biomed. Health*., **25** (2021), 47–58. https://doi.org/10.1109/JBHI.2020.2987528
53. D. L. Donoho, De-noising by soft-thresholding, *IEEE Trans. Inf. Theory*, **41** (1995), 613–627. https://doi.org/10.1109/18.382009
54. H. Ashraf, A. Waris, S. O. Gilani, M. U. Tariq, H. Alquhayz, Threshold parameters selection for empirical mode decomposition-based EMG signal denoising, *Intell. Autom. Soft Comput*., **27** (2021), 799–815. https://doi.org/10.32604/iasc.2021.014765
55. S. Phatak, S. S. Rao, Logistic map: A possible random-number generator, *Phys. Rev. E*, **51** (1995), 3670. https://doi.org/10.1103/PhysRevE.51.3670

56. L. Kahl, U. G. Hofmann, Comparison of algorithms to quantify muscle fatigue in upper limb muscles based on sEMG signals, *Med. Eng. Phys*., **38** (2016), 1260–1269. https://doi.org/10.1016/j.medengphy.2016.09.009
57. Y. X. Li, B. Z. Tang, B. Geng, S. B. Jiao, Fractional order fuzzy dispersion entropy and its application in bearing fault diagnosis, *Fractal Fract*., **6** (2022), 544. https://doi.org/10.3390/fractalfract6100544
58. E. Z. Song, Y. Ke, C. Yao, Q. Dong, L. P. Yang, Fault diagnosis method for high-pressure common rail injector based on IFOA-VMD and hierarchical dispersion entropy, *Entropy*, **21** (2019), 923. https://doi.org/10.3390/e21100923
59. X. A. Yan, Y. D. Xu, M. P. Jia, Intelligent fault diagnosis of rolling-element bearings using a self-adaptive hierarchical multiscale fuzzy entropy, *Entropy*, **23** (2021), 1128. https://doi.org/10.3390/e23091128
60. R. J. Zhou, X. Wang, J. Wan, N. X. Xiong, EDM-Fuzzy: An Euclidean distance based multiscale fuzzy entropy technology for diagnosing faults of industrial systems, *IEEE Trans. Ind. Inf*., **17** (2021), 4046–4054. https://doi.org/10.1109/TII.2020.3009139
61. A. Shoeibi, N. Ghassemi, M. Khodatars, P. Moridian, A. Khosravi, A. Zare, et al., Automatic diagnosis of schizophrenia and attention deficit hyperactivity disorder in RS-fMRI modality using convolutional autoencoder model and interval type-2 fuzzy regression, *Cognit. Neurodyn*., **17** (2023), 1501–1523. https://doi.org/10.1007/s11571-022-09897-w
62. H. M. Qassim, W. Z. W. Hasan, H. R. Ramli, H. H. Harith, L. N. I. Mat, L. I. Ismail, Proposed fatigue index for the objective detection of muscle fatigue using surface electromyography and a double-step binary classifier, *Sensors*, **22** (2022), 1900. https://doi.org/10.3390/s22051900
63. K. D. Bharathi, P. A. Karthick, S. Ramakrishnan, Automated detection of muscle fatigue conditions from cyclostationary based geometric features of surface electromyography signals, *Comput. Methods Biomech. Biomed. Eng.*, **25** (2022), 320–332. https://doi.org/10.1080/10255842.2021.1955104
64. N. Makaram, P. A. Karthick, V. Gopinath, R. Swaminathan, Surface Electromyography-based muscle fatigue analysis using binary and weighted visibility graph features, *Fluctuation Noise Lett*., **20** (2021), 2150016. https://doi.org/10.1142/S0219477521500164
65. D. B. Krishnamani, P. A. Karthick, R. Swaminathan, Variational mode decomposition based differentiation of fatigue conditions in muscles using surface electromyography signals, *IET Signal Process*., **14** (2021), 745–753. https://doi.org/10.1049/iet-spr.2020.0315
66. D. Sasidharan, V. Gopinath, R. Swaminathan, A proposal to analyze muscle dynamics under fatiguing contractions using surface Electromyography signals and fuzzy recurrence network features, *Fluctuation Noise Lett*., **22** (2023), 2350033. https://doi.org/10.1142/S0219477523500335
67. D. Sasidharan, V. Gopinath, R. Swaminathan, Complexity analysis of surface Electromyography signals under fatigue using Hjorth parameters and bubble entropy, *J. Mech. Med. Biol*., **23** (2023), 2340051. https://doi.org/10.1142/S0219519423400511
68. A. Greco, G. Valenza, A. Bicchi, M. Bianchi, E. P. Scilingo, Assessment of muscle fatigue during isometric contraction using autonomic nervous system correlates, *Biomed. Signal Process*., **51** (2019), 42–49. https://doi.org/10.1016/j.bspc.2019.02.007

69. W. D. Wang, H. H. Li, D. Z. Kong, M. H. Xiao, P. Zhang, A novel fatigue detection method for rehabilitation training of upper limb exoskeleton robot using multi-information fusion, *Int. J. Adv. Robot Syst*., **17** (2020), 1–11. https://doi.org/10.1177/1729881420974295
70. S. R. Wang, H. Tang, B. Wang, J. Mo, A novel approach to detecting muscle fatigue based on sEMG by using neural architecture search framework, *IEEE Trans. Neural Network Learn*., **34** (2023), 4932–4943. https://doi.org/10.1109/TNNLS.2021.3124330
71. S. K. Chen, K. L. Xu, X. W. Yao, J. Ge, L. Li, S. Y. Zhu, et al., Information fusion and multi-classifier system for miner fatigue recognition in plateau environments based on electrocardiography and electromyography signals, *Comput. Methods Programs Biomed*., **211** (2021), 106451. https://doi.org/10.1016/j.cmpb.2021.106451
72. S. K. Chen, K. L. Xu, X. W. Yao, S. Y. Zhu, B. H. Zhang, H. D. Zhou, et al., Psychophysiological data-driven multi-feature information fusion and recognition of miner fatigue in high-altitude and cold areas, *Comput. Biol. Med*., **133** (2021), 104413. https://doi.org/10.1016/j.compbiomed.2021.104413
73. Q. Liu, Y. Liu, C. S. Zhang, Z. L. Ruan, W. Meng, Y. L. Cai, et al., SEMG-based dynamic muscle fatigue classification using SVM with improved whale optimization algorithm, *IEEE Int. Things*, **8** (2021), 16835–16844. https://doi.org/10.1109/JIOT.2021.3056126
74. J. X. Liu, Q. Tao, B. Wu, Dynamic muscle fatigue state recognition based on deep learning fusion model, *IEEE Access*, **11** (2023), 95079–95091. https://doi.org/10.1109/ACCESS.2023.3309741
75. J. R. Suganthi, K. Rajeswari, Evaluation of muscle fatigue based on SEMG using deep learning techniques, in *2023 5th International Conference on Inventive Research in Computing Applications (ICIRCA)*, (2023), 1–6. https://doi.org/10.1109/ICIRCA57980.2023.10220926
76. Y. Q. Zhang, S. Y. Chen, W. P. Cao, P. Guo, D. R. Gao, M. Q. Wang, et al., MFFNet: Multi-dimensional feature fusion network based on attention mechanism for sEMG analysis to detect muscle fatigue, *Exp. Syst. Appl*., **185** (2021), 115639. https://doi.org/10.1016/j.eswa.2021.115639
77. Y. K. Dang, Z. T. Liu, X. X. Yang, L. Q. Ge, S. Miao, A fatigue assessment method based on attention mechanism and surface electromyography, *Int. Things Cyber-Phys. Syst*., **3** (2023), 112–120. https://doi.org/10.1016/j.iotcps.2023.03.002

AIMS Press